FEASIBILITY OF NON-INVASIVE OSR DIAGNOSTICS IN THE AWAKE RUN-2C INJECTION REGION

D. Ghosal[1,2,*], J. Wolfenden[1,2], M. Turner[3], C. P. Welsch[1,2], AWAKE Collaboration
[1]Department of Physics, University of Liverpool, Liverpool, UK
[2]Cockcroft Institute, Warrington, UK
[3]European Organization for Nuclear Research, Geneva, Switzerland

Abstract

AWAKE experiment at CERN is currently advancing toward Run-2c to demonstrate the higher energy acceleration of electrons while maintaining the beam quality. A second electron beam (of 150 MeV energy) will be injected and accelerated to several GeVs while aiming to keep good emittance. Diagnostics are being upgraded for this geometrically constrained injection-region to enable single-shot characterization of that beam, among which this contribution evaluates the feasibility of optical synchrotron radiation as a non-invasive real-time mean. It can provide shot-by-shot transverse position and profile information without disrupting beam delivery, critical for benchmarking beam-alignment and quality check. The prompt, non-invasive nature also makes it a candidate for future virtual diagnostic implementations, where online beam profiles could inform predictive models or feedback correction schemes. For performance optimizations the expected photon flux, photon statistics, projected image quality are computed with realistic imaging optics and detector quantum efficiency. Results demonstrate that sufficient signal can be extracted through this compact optical chain to achieve the target.

INTRODUCTION

Plasma wakefield acceleration (PWFA) has emerged as a promising route toward compact, high-gradient particle accelerators, achieving accelerating gradients orders of magnitude beyond conventional RF technology [1, 2]. However, the extreme field strengths and complex beam-plasma dynamics in PWFA demand advanced diagnostics capable of characterizing beam quality shot-by-shot without disrupting acceleration. AWAKE (Advanced Wakefield Experiment) is CERN's pioneering facility for proton-driven PWFA, exploiting the high energy density of the Super Proton Synchrotron (SPS) beam to drive wakefields in plasma column, depicted in Fig. 1. Over the past years AWAKE successfully demonstrated the self-modulation of the proton driver and the acceleration of externally injected electrons over a 10-meter plasma [3]. These proof-of-principle results established the viability of higher-quality beam acceleration.

The current AWAKE program is advancing towards the third phase of Run-2 [4], which aims to inject and accelerate a witness electron bunch from 150 MeV to multi-GeV energies while maintaining low emittance. However, any injection error in position, angle, or beam size can lead to

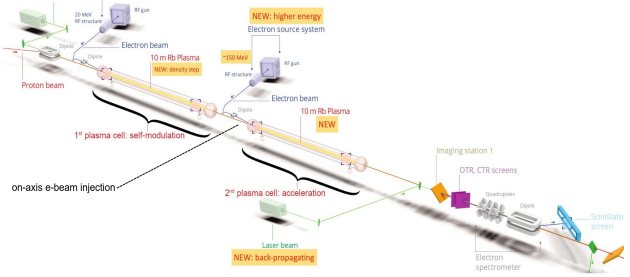

Figure 1: Schematic of AWAKE beamline [3].

emittance growth, reduced acceleration efficiency, or beam loss. As a result, characterizing the witness beam immediately upstream of the second plasma cell entrance is essential for injection alignment verification, shot-to-shot stability monitoring, machine optimization and finally benchmarking simulations. Instead of traditional diagnostics [5, 6] which are not very suitable for online monitoring due to their invasive nature and demand of a multiple measurements, non-invasive real-time beam monitoring are superior for single shot characterization, and critical to understand the initial beam properties entering the plasma, that directly influence acceleration efficiency and overall performance.

Optical synchrotron radiation (OSR), the visible and near-UV portion of the photons spectra (emitted when relativistic electrons traversing in a magnetic field), has emerged as such a powerful non-invasive diagnostic over the years [7, 8]. For AWAKE Run-2c, the dipole in the injection beamline presents an opportunity to extract OSR from the 150 MeV electron beam. However, the region is geometrically constrained by vacuum chambers, limited viewport apertures, and a buffer gas region required for vacuum isolation from the plasma source. The comparatively lower critical photon energy (E_c) at 150 MeV demands careful evaluation of photon yield and detection feasibility. This paper evaluates the physics feasibility of using OSR from the injection dipole for the upcoming the Run-2c as a non-invasive, single shot transverse profile measurement.

EXTRACTION GEOMETRY AND SIMULATION FRAMEWORK

A key parameter E_c dictates approximately half of the total radiated power is emitted above and half below it, with the spectrum extending from the near-IR through the UV. Considering a bending radius of $\rho \sim 1.0$m of the injection

* dghosal@liverpool.ac.uk

dipole

$$E_c = \frac{3\hbar c\gamma^3}{2\rho} \approx 7eV \quad (1)$$

The angular distribution of synchrotron radiation (SR) is characterized by the opening angle: $\theta_{\text{cone}} \sim 1/\gamma$ ($\approx$ 3.4mrad for 150 MeV beam), while approximately 95% of the emitted radiation is contained within a cone of opening angle $\sim 3/\gamma$.

Beyond the angular distribution, SR also exhibits characteristic polarization structure that can be exploited for diagnostic purposes. These properties depend on observation angle relative to the orbital plane; σ-polarization (s-pol) dominates for on-axis observation (electric field vector oscillates perpendicular to the orbital plane) and π-polarization (p-pol) is for the off-axis observation i.e. the electric field oscillates in the plane [9].

Geometric Acceptance

The optical extraction path in the AWAKE electron injection area is quite constrained by the beamline geometry. At a distance of 45 cm from the dipole source, a 15 mm diameter aperture of the DN16 viewport subtends a half-angle of $\theta_{\text{aperture}} \approx 16.7$ mrad. This aperture acceptance angle is larger than the characteristic SR cone ($1/\gamma$) and even exceeds the $3/\gamma \approx 10$ mrad cone containing most of the radiated power. But a quantitative acceptance calculations can be further confirmed by comparing the solid angles subtended by the aperture and the SR emission cone (next section).

However, photon transmission can also be affected by the argon-filled buffer region between DN16 and DN40. Argon exhibits strong absorption for wavelengths below $\sim$ 105 nm (photon energies above ~11.8 eV) due to photoionization [10], but is relatively transparent in the 105–-400-nm range where the bulk of the 150 MeV OSR spectrum resides. For the primary OSR band centered around $E_c \approx 7-8$ eV ($\lambda \approx$ 155–177 nm), argon transmission is expected to be favorable, though some attenuation might occur for the high-energy UV tail of the spectrum. Once collected, the OSR diagnostic provides access to key beam parameters like- transverse beam position (centroid), beam profile and indirectly trajectory angle, providing continuous feedback for machine optimization and serving as a baseline for comparison with post-acceleration beam properties measured downstream. Shot-to-shot centroid tracking enables monitoring of injection stability and alignment. The OSR image also encodes the transverse charge distribution of the electron beam, convolved with the single-electron SR angular distribution. For beam size comparable to or larger than the single-electron SR spot size), the profile measurement provides valuable size and shape information.

SR Model and Propagation

The spectral-angular distribution of SR can be calculated analytically using the standard formalism based on modified Bessel functions. For this study, we employ the Synchrotron Radiation Workshop (SRW) code [11], which computes the electromagnetic field using frequency-domain methods from the Fourier-transformed retarded potentials and evaluates the transverse electric field components at the observation point, accounting for both near-field and far-field effects [12].

Having calculated the SR emission characteristics, the propagation of this radiation through the constrained beamline geometry was modeled. For each electron in the bunch, photons are generated according to the spectral-angular distribution and propagated through the geometry. The solid angle acceptance is:

$$\Omega_{\text{aperture}} = \pi \left(\frac{r_{\text{DN16}}}{d_{\text{source-DN16}}} \right)^2 \approx 2.77 \times 10^{-4} sr \quad (2)$$

Compared to the SR emission solid angle: $\Omega_{SR} = \pi(3/\gamma)^2 \approx 3.27 \times 10^{-4} sr$. The ratio $\Omega_{\text{aperture}}/\Omega_{SR} \approx 0.85$ confirms that the DN16 aperture captures approximately 85% of the SR cone, while the following larger DN40 window introduces no additional losses.

Beyond that OSR photons pass through additional optical elements before reaching the detector. In regards to the filter usage, broadband operation maximizes photon flux, while narrowband filtering reduces background from stray visible light and plasma emission at the cost of reduced signal. Furthermore, mirrors to be used to direct OSR from the DN40 exit window to the camera. Assuming aluminum-coated mirrors in the relay optics, for a two-mirror relay system, total reflectivity is $R_1 \times R_2 \approx 0.5$–$0.75$ depending on wavelength. Having established the individual transmission and reflection coefficients for each optical element, the cumulative total transmission from source to detector is the product of all wavelength-dependent losses along the optical path:

$$T_{\text{total}} = T_{\text{buffer}}(\lambda) \times T_{\text{filter}}(\lambda) \times R_{\text{mirrors}} \times T_{\text{window}} \quad (3)$$

Although the SR critical wavelength is in the UV range ($\lambda_c \approx$ 155–165 nm), the photon number spectrum is weighted toward longer wavelengths due to the λ dependence of photon energy. As a result, the detected signal is dominated by visible and near-IR photons, where the transmission of optical components and detector quantum efficiency are significantly higher.

Imaging System and Photon Statistics

A critical optical design consideration will ensure adequate pixel sampling of the OSR angular distribution. The SR emission cone projects to different image sizes depending on focal length. Key design trade-offs will be among resolution, field of view, and working distance.

For a nominal bunch charge of 100 pC (corresponding to $N_e \approx 6.24 \times 10^8$ electrons), the total number of photons emitted per bunch is: $N_{\gamma,\text{total}} \sim 10^3 \times 6.24 \times 10^8 \approx 10^{11}$. However, only a certain amount of these photons falls within the optical band (400–800 nm) relevant for detection typically of the order 10^{-3}–10^{-2}, yielding: $N_{\gamma,\text{optical}} \sim 10^8 - 10^9$.

Now expected signal levels and actual photon statistics at the detector can be calculated by geometric acceptance,

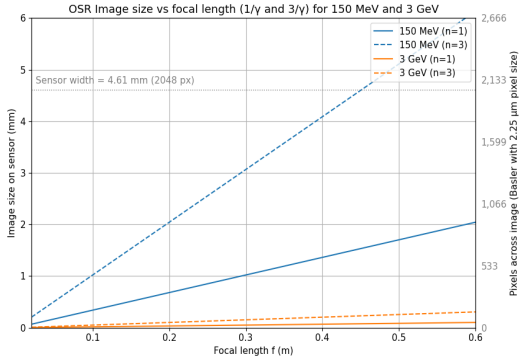

Figure 2: Image size on sensor vs. focal length, showing number of Basler camera pixels (2.25 µm pitch) across the SR image.

optical transmission losses, and detector quantum efficiency.

$$N_{\text{detected}} = N_{\gamma,\text{optical}} \times T_{\text{tot}} \times QE \times f_{\text{coll}} \sim 10^7 - 10^8 \quad (4)$$

Distributed over an image of a few hundred pixels (depending on beam size and magnification, such as Fig. 2), this yields: $N_{\text{photons/pixel}} \approx 10^4$–$10^6$. The shot noise becomes: $\sigma_{\text{shot}} = \sqrt{N} \sim 10^4$–$10^5$ Yielding a signal-to-noise ratio:

$$SNR = N/\sigma_{\text{shot}} \sim 10^2\text{–}10^3$$

This excellent SNR enables high-precision centroid and profile measurements even on single shot cases.

PERFORMANCE ASSESSMENT

The subplots in Fig. 3 show the calculated OSR spectrum for the 150 MeV beam showing photon flux vs photon energy. The spectrum peaks around 2–3 eV (~400-600 nm) with the critical energy $E_c \approx 7.5$ eV (165 nm) marking the halfway point of the radiated power. The fairly broad spectral distribution provides flexibility in filter selection: broadband imaging captures maximum signal, even with narrowband filtering, photon statistics remain fine (very good SNR).

The two subfigures in Fig. 4 display the geometric acceptance and the angular distribution of the accepted photons respectively. A fraction of large-angle emission is clipped by the apertures, resulting in an estimated geometric acceptance of ~ 85% based on solid angle considerations of $(3/\gamma)$. Furthermore, SR is peaked near ~ $1/\gamma$ and fewer photons

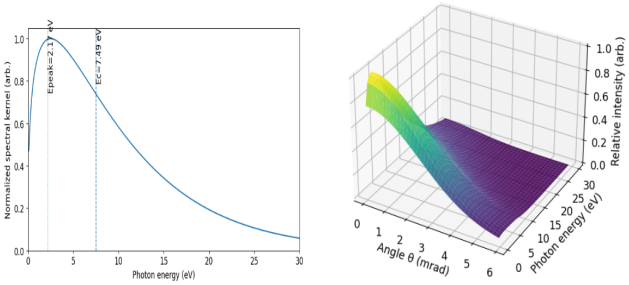

Figure 3: The photon energy scan (left subplot) and the 3D angular distribution (the same energy scan with intensity and angle (angular observation coordinate)).

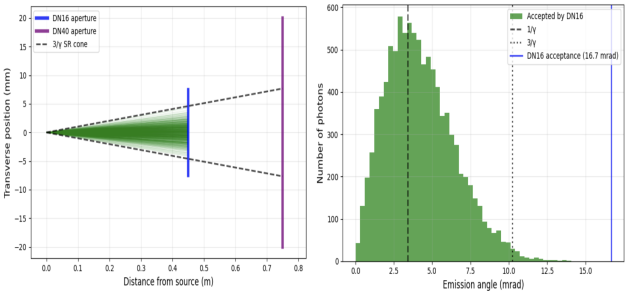

Figure 4: Left subfigure is the side view of the accepted photons propagation through the two apertures, while the right subfigure shows the angular distribution of the accepted photons, the vertical lines: $1/\gamma \approx 3.4$ mrad, $3/\gamma \approx 10$ mrad.

at large angles i.e. the lost region (large θ) contains less intensity.

Lastly, the large photon count ensures that beam profiles will be well resolved with high statistical precision on single shots. The detected photon flux scales linearly with bunch charge ($N_{\text{detected}} \propto Q$), in the absence of detector saturation or other non-linear effects. For a nominal $Q = 100$ pC (6.24×10^8 electrons), we obtain ~ 10^7–10^8 detected photons. This scaling implies ~ 10^6–10^7 photons for $Q = 50$ pC, corresponding to a SNR ratio still above 100. Hence, the diagnostic remains viable across the expected operational range, with comfortable margins even at reduced charge.

Finally, there will be trade-offs regarding the magnification of the optical system. A magnification of $M \approx 0.5$–1 is recommended to balance spatial resolution, field of view, and photon statistics per pixel, while avoiding excessive magnification that can complicate the optical layout and working distance. Care must also be taken to avoid detector saturation at higher photon flux.

CONCLUSION

To conclude, we have evaluated the feasibility of OSR as a non-invasive, single-shot beam profile-diagnostic for the 150 MeV electron injection line in AWAKE Run-2c. Despite the challenging constraints such as lower beam energy ($E_c \approx$ few eV), tight geometric apertures and space-constrained beamline area, the analysis demonstrates that OSR-based beam monitoring is both feasible and practical. Key findings are: sufficient photon yield, excellent SNR, operational robustness and complementary diagnostic capability and beam profile measurements with 5–10% resolution, providing flexibility for commissioning and optimization. The non-invasive nature and high photon statistics position this diagnostic as a candidate for future virtual diagnostic implementations, where injection beam profiles could inform predictive models or enable per shot feedback correction of upstream parameters if injection optimization is required.

ACKNOWLEDGEMENTS

This work was supported by the AWAKE-UK phase II project funded by STFC under grant No. ST/X005208/1.

REFERENCES

[1] M. Litos *et al.*, "High-efficiency acceleration of an electron beam in a plasma wakefield accelerator", *Nature*, vol. 515, pp. 92–95, 2014. doi:10.1038/nature13882.

[2] P. Muggli, "Beam-driven, plasma-based particle accelerators", in *Proc. CAS-CERN Accelerator School: Plasma Wake Acceleration*, Geneva, Switzerland, November 2014, pp. 119–142. doi:10.5170/CERN-2016-001.119

[3] Edda Gschwendtner, "The AWAKE Experiment", in *UK-CERN Accelerator Celebration Day*, Daresbury, UK, Nov. 27, 2025. https://indico.global/event/15484/contributions/139281/attachments/64874/125523/2025-11-27-CERN-UK-AWAKE.pdf

[4] R. Ramjiawan *et al.*, "Design of the proton and electron transfer lines for AWAKE Run 2c", *Nuclear Inst. and Methods in Physics Research, A*, vol. 1049, 2023. doi:10.1016/j.nima.2023.168094

[5] M. Wendt, "Challenges in Accelerator Beam Instrumentation", in *Proc. of DPF-2009*, Detroit, MI, July 2009. https://lss.fnal.gov/archive/2009/conf/fermilab-conf-09-670-ad.pdf

[6] H. Zhang, "Beam diagnostics (destructive methods)", *AVA school on Low Energy Antimatter Physics*, CERN, Geneva, Switzerland, Rep. June 2018. https://indico.cern.ch/event/677170/contributions/2772376/attachments/1674153/2687096/beam_diagnostic_destructive_method.pdf

[7] R. H. A. Farias *et al.*, "Optical beam diagnostics for the LNLS synchrotron light source", in *Proc. PAC'97*, Vancouver, BC, Canada, pp. 2238–2240, 1997. doi:10.1109/PAC.1997.751168

[8] R. Thurman-Keup *et al.*, "Synchrotron radiation based beam diagnostics at the Rermilab Tevatron", *J. Instrum.*, vol. 6, no. 9, p. T09003, 2011. doi:10.1088/1748-0221/6/09/T09003

[9] M. Dohlus *et al.*, "Application of Accelerators and Storage Rings", *Particle Physics Reference Library*, pp. 661–795, May 2020. doi:10.1007/978-3-030-34245-6$_$11

[10] R. E. Huffman, J. C. Larrabee, and Y. Tanaka, "Absorption Coefficients of Argon in the 600–1100 Å Region", *The Journal of Chemical Physics*, vol. 39, no. 4, pp. 902–909, 1963. doi:10.1063/1.1734390

[11] ESRF-SRW, "Synchrotron radiation workshop", https://www.esrf.fr/Accelerators/Groups/InsertionDevices/Software/SRW

[12] O. Chubar *et al.*, "Accurate and efficient computation of synchrotron radiation in the near field region", in *Proc. EPAC'98*, Stockholm, Sweden, Jun. 1998, paper THP01G, pp. 1177–1179.